厚生労働科学研究費補助金

障害者対策総合研究事業

動脈ラベル標識法（ASL）を用いた精神疾患の脳画像解析法の確立に関する研究

平成23年度～平成25年度　総合研究報告書

研究代表者　太田深秀

平成 26（2014）年　4 月

目　　次

厚生労働科学研究費補助金（障害者対策総合研究事業）
（総合）研究報告書

動脈ラベル標識法（ASL）を用いた精神疾患の脳画像解析法の確立に関する研究

研究代表者　太田　深秀　国立精神・神経医療研究センター神経研究所
疾病研究第三部　室長

研究要旨

近年3テスラのMRIの普及に伴いASLによる局所脳血流量測定が注目されている。そこで我々はうつ病や統合失調症などを対象とした精神疾患の脳データーバンクの作成を行い、脳形態画像とASLとを組み合わせた新しい精神疾患の客観的診断法を確立することを目的とする。

太田　深秀
国立精神・神経医療研究センター神経研究所疾病研究第三部　室長

A．研究目的

近年の研究により、精神疾患における局所脳変化が明らかになってきている。また形態学的変化のみならず、これまでSPECTやPETを用いた脳血流検査を対象とした疾患研究でも精神疾患患者における特異な変化が確認されている。我々は
pseudo-continuous arterial spin labelingを用いた非侵襲的な手法によって精神疾患患者の脳血流変化を検証した。。

B．研究方法

当センターでそれぞれ大うつ病性障害、統合失調症、双極性障害および健常と診断された方を対象に被験者を対象に3TのMRIによりT1強調画像、pCASLによる脳血流画像を撮影した。

（倫理面への配慮）

対象者には検査に関する説明を行い、文書にて同意を得た。

C．研究結果

大うつ病性障害患者では帯状回膝下部などにおける脳血流低下を確認しており、PETやSPECTを用いた先行論文で指摘されている障害部位と合致した。この結果は大うつ病性障害患者と統合失調症患者を比較した時も有意であった。一方統合失調症患者群では左下前頭前野の血流低下が認められており、先行の核医学的手法にて明らかとなった統合失調症における局所脳血流変化と合致した結果であった。

D．考察

これらの結果はPETやSPECTを用いた先行論文で指摘されている障害部位と合致しており、pCASLによる脳血流検査が従来の核医学検査と同程度の有用性を持つことが示唆された。

E.結論

平成23年度から始まった当研究では、pCASLの定量解析方法の確立から始まり平成24年度には多発性硬化症や統合失調症の脳血流変化を明らかとした。平成25年度には大うつ病性障害における血流変化を明らかにした。これまでに300名程度の撮像を終了しており、サンプル数の確保としては当初の目的は達成できた。今後は各疾患における重症度判定などの方法論の確立を行いつつ、データーベースの構築などを行う。

F.研究発表

1.　論文発表

Ota M et al: Magnetic Resonance Imaging 31: 990-995.
Ota M et al: Brain Research 1499:61-68, 2013.
Ota M et al: J Psychiatr Res 47:1383-1388, 2013.
Ota M et al: Schizophr Res, 2014 (in press)

2.　学会発表

現在投稿準備中

H．知的財産権の出願・登録状況

1．特許取得

予定なし

2．実用新案登録

予定なし

研究成果の刊行に関する一覧表レイアウト

書籍

著者氏名	論文タイトル名	書籍全体の編集者名	書　籍　名	出版社名	出版地	出版年	ページ
該当なし							

雑誌

発表者氏名	論文タイトル名	発表誌名	巻号	ページ	出版年
Miho Ota et al	Neuroimaging study in subjects at high risk of psychosis revealed by the Rorschach test and first-episode schizophrenia	Acta Neuropsychiatrica	23	125-131	2011
Miho Ota et al	A polymorphism of the ABCA1 gene confers susceptibility to schizophrenia and related brain changes	Prog Neuropsychopharmacol Biol Psychiatry	35	1877-1883	2011
Miho Ota et al	Abnormalities of cerebral blood flow in multiple sclerosis: A pseudocontinuous arterial spin labeling MRI study	Magnetic Resonance Imaging	31	990	2013
Miho Ota et al	Multimodal image analysis of sensorimotor gating in healthy women.	Brain Research	1499	61-68	2013
Miho Ota et al	Discrimination between schizophrenia and major depressive disorder by magnetic resonance imaging of the female brain.	J Psychiatr Res	47	1383	2013
Miho Ota et al	Pseudo-continuous arterial spin labeling MRI study of schizophrenic patients.	Schizophr Res	In press		2014

Acta Neuropsychiatrica

Acta Neuropsychiatrica 2011: 23: 125–131
All rights reserved
DOI: 10.1111/j.1601-5215.2011.00547.x

ACTA NEUROPSYCHIATRICA

Neuroimaging study in subjects at high risk of psychosis revealed by the Rorschach test and first-episode schizophrenia

Ota M, Obu S, Sato N, Asada T. Neuroimaging study in subjects at high risk of psychosis revealed by the Rorschach test and first-episode schizophrenia.

Objective: There is increasing evidence of neuroanatomical pathology in schizophrenia, but it is unclear whether changes exist prior to disease onset. This study aimed to examine whether changes exist prior to disease onset, especially in the temporal lobes.
Methods: T1-weighted and diffusion tensor magnetic resonance imaging were performed on 9 first-episode schizophrenia patients, 10 patients who were at high risk of schizophrenia and 10 healthy controls. Voxel-based analysis using the normalised images of cortical volume data was examined, and the fractional anisotropy value at three component fibres of the temporal lobes, inferior longitudinal fasciculus, superior longitudinal fasciculus (SLF) and cingulum hippocampal part was compared among the three groups.
Results: There were statistically significant volume differences at the bilateral temporal lobe between the healthy subjects and high-risk group. Between the schizophrenic group and healthy subjects, statistically significant volume differences were detected at the bilateral temporal lobes and anterior cingulate cortex. The fractional anisotropy values of the SLF in the schizophrenic and high-risk groups were significantly lower than in the healthy subjects.
Conclusion: Our findings indicate that some brain alterations may progress in patients at psychosis pre-onset, possibly because of disrupted developmental mechanisms, and these pathological changes may be predictive of functional outcome.

Miho Ota[1,2], Satoko Obu[2], Noriko Sato[1], Takashi Asada[3]

[1]Department of Radiology, National Center of Neurology and Psychiatry, Kodaira, Tokyo, Japan; [2]Department of Psychiatry, Hospital Bando, Bando, Ibaraki, Japan; and [3]Department of Neuropsychiatry, Institute of Clinical Medicine, University of Tsukuba, Tsukuba, Ibaraki, Japan

Keywords: diffusion tensor imaging; magnetic resonance imaging; Rorschach test; schizophrenia; voxel-based morphometry

Miho Ota, Department of Radiology, National Center of Neurology and Psychiatry, 4-1-1, Ogawa-Higashi, Kodaira, Tokyo 187-8551, Japan.
Tel: +81 42 341 2711;
Fax: +81 42 346 2094;
E-mail: ota@ncnp.go.jp

Introduction

Structural brain abnormalities have consistently been shown to be present in people with schizophrenia (1–3), and how the brain abnormalities observed in schizophrenia develop is of great interest. Some behavioural features can be observed in patients with schizophrenia years before the onset of illness (4,5), suggesting that there are neural differences from a very early age that may make these individuals more vulnerable to later insults. Early detection and prevention strategies for schizophrenia have led to investigations of individuals at the high risk of psychosis, who present with a constellation of clinical symptoms thought to be characteristic of the psychosis in the 'prodromal period', when the onset of schizophrenia would be expected to occur. Such studies seek to characterise the developmental processes that lead to disturbances of the brain structure and function associated with the onset of psychosis, and to find baseline traits that are predictive of later diagnostic conversion or functional decline. Previous studies mainly used the PACE criteria for the identification of those high risk of development psychosis (6). However, the previous neuroimaging studies adopting showed inconsistent results (7–11).

The Rorschach test has been used historically as a way to identify psychological processes associated

with thought and perceptual disturbance, and to aid in the differential diagnosis of schizophrenia. For the differential diagnosis, the Perceptual Thinking Index (PTI) comprised of eight Rorschach variables that are arranged based on a combination of different values on five empirical criteria was developed (12,13). It measures both perceptual oddities and cognitive slippage, and sufficient (Intraclass Correlation Coefficient >0.8) reliability and validity was also investigated (14). This supports the notion of applying it to the detection of psychosis risk in a clinical population. The preceding studies showed that individuals at clinical high risk for psychosis established using the Structured Interview for Prodromal Symptoms and the Scale of Prodromal Symptoms (SIPS/SOPS; 15) displayed substantial deficits in visual form perception prior to the onset of psychosis revealed by Rorschach test (16,17). Ilonen et al. showed that the PTI distinguished patients at clinical high risk for psychosis from those diagnosed as having non-psychotic disorders (16). The deficits in visual form perception revealed by the PTI fell under the group 1; the attenuated psychotic symptoms of the PACE criteria. In this study, we used the PTI to evaluate patients without delusion, hallucination and catatonic behaviour, but at high-risk mental state for schizophrenia.

Previous cross-sectional imaging studies in schizophrenia found reduced grey matter volume compared to controls, particularly in the temporal lobes, and some studies showed that there were significant differences in temporal lobes between the healthy subjects and pre-onset or at high genetic risk of schizophrenia groups (11,18,19). However, no study investigated the impairment of the component fibres at temporal regions coupled with volume data. In this study, therefore, we first evaluated the cortical volume difference among the pre-onset group, first-episode schizophrenic group and healthy controls. We then investigated the microstructural change among the three groups at three component fibres of the temporal lobes, the inferior longitudinal fasciculus (ILF), superior longitudinal fasciculus (SLF) and cingulum hippocampal part that runs along the ventral aspect of the hippocampus.

Method

Subjects

Five male and four female first-episode schizophrenia patients, defined according to the criteria described in the fourth edition of the *Diagnostic and Statistical Manual of Mental Disorders* (DSM-IV), were recruited at Hospital Bando (Ibaraki, Japan). Their mean age was 29.0 ± 4.3 years (ranging from 23 to 34 years). Only one patient was drug naive, while the other eight were being treated with antipsychotic medication. The mean interval between the first patient contact and magnetic resonance imaging (MRI) scan was 33.9 ± 21.7 days (ranging from 0 to 70 days).

We also recruited patients who were regarded as having a clinical high risk for schizophrenia but who did not fulfill the schizophrenia criteria. Patients showing the presence of at least one of the following symptoms were tested with the Rorschach test: ideas of reference, magical thinking, perceptual disturbance, paranoid ideation, odd thinking and speech. The individual PTI was scored, and a score of $\geqq 1$ was regarded as showing perceptual disturbance (16). As a consequence, four male and six female patients (mean age 25.5 ± 11.1 years, ranging from 16 to 46 years, mean PTI score 3.6 ± 0.8) were regarded as at high risk for the developing psychosis.

Exclusion criteria included a history of head injury, neurological symptoms, speech or hearing difficulties, significant cerebrovascular diseases (cortical infarctions, multiple lacunar lesions or leukoaraiosis) and fulfilment of the DSM-IV criteria for abuse of illicit drugs or alcohol at any point during their lifetime.

Ten sex- and age-matched healthy subjects (four males and six females, mean age 26.1 ± 3.8 years, ranging from 16 to 30 years) were also included in the study.

All participants provided their written informed consent, and the local ethics committee approved the study protocol.

Data acquisition and processing

MRI was performed on a 1.5 Tesla Siemens Magnetom Harmony (Erlangen Germany). Diffusion tensor imaging (DTI) was carried out on the axial plane (echo time (TE)/repetition time (TR) = 100/7000 ms; field of view (FOV), 262 × 262 mm; matrix 128 × 128; 40 continuous transverse slices; slice thickness, 4 mm with no slice gap). To enhance the signal-to-noise ratio, acquisition was repeated four times. Diffusion was measured along 12 non-collinear directions with the use of a diffusion-weighted factor *b* in each direction of 1000 s/mm^2, and one image was acquired without the use of a diffusion gradient. High-spatial-resolution, 3-dimensional (3D) T1-weighted images of the brain were obtained for morphometric study. 3D T1-weighted images were scanned on the sagittal plane [TE/TR, 3.93/1460 ms; flip angle, 15°; effective section thickness, 1.5 mm; slab thickness, 168 mm; matrix, 256 × 256; FOV, 250 × 250; 1 number of excitations (NEX)], yielding 112 contiguous slices through the head. In addition to DTI and 3D T1-weighted images, we also acquired

axial T2-weighted turbo spin echo images (TE/TR, 95/3800 ms; slice thickness, 6 mm; intersection gap, 1.2 mm; matrix, 384 × 288; FOV, 220 × 175 mm; acquisition, 1) and fluid attenuation inversion recovery (FLAIR) images on the axial plane (TE/TR, 104/9000 ms; flip angle, 170°; slice thickness, 6 mm; intersection gap, 1.2 mm; matrix, 256 × 192; FOV, 220 × 175 mm; acquisition, 1) to rule out cerebral vascular disease.

The raw diffusion tensor and 3D T1-weighted volume data were transferred to the workstation and the DTI data sets were analysed using DtiStudio (H. Jiang and S. Mori; Johns Hopkins University). The diffusion tensor parameters were calculated on a pixel-by-pixel basis, and the FA map, $b = 0$ image and finally 3D fibre tracts were calculated (20).

To clarify volume differences among the two patient groups and healthy subjects, structural 3D T1-weighted MR images were analysed using an optimised voxel-based morphometry (VBM) technique. Data were analysed using Statistical Parametric Mapping 5 (SPM5) software (Welcome Department of Imaging Neuroscience, London, UK) running on MATLAB 7.0 (Math Works, Natick, MA, USA). Images were processed using optimised VBM script. Details of this process are described elsewhere (21). Normalised segmented images were modulated by multiplication with Jacobian determinants of spatial normalisation function to encode the deformation field for each subject as tissue density changes in normal space. Images were smoothed using an 8-mm full-width half-maximum of an isotropic Gaussian kernel.

To exclude some of the subjectivity involved in defining regions of interest (ROIs), we made fibre ROIs normalised to the standard space, and then placed the ROIs on all of the individual FA images normalised to the standard space for the evaluation of FA. First, each individual 3D-T1 image was coregistered and resliced to its own $b = 0$ image. Next, the coregistered 3D-T1 image was normalised to the 'avg152T1' image regarded as the anatomically standard image in SPM5. Finally, the transformation matrix was applied to the FA map. Each map was then spatially smoothed by a 6-mm full-width half-maximum Gaussian kernel in order to decrease spatial noise and compensate for the inexact nature of normalisation following the 'rule of thumb' developed for functional MRI and positron emission tomography studies (22).

Fibre tractography was performed on the data of 10 healthy subjects with a threshold value of fibre-tracking termination of FA = 0.2 and a trajectory angle of 50° (23). The definition of the bilateral ILF, SLF and cingulum hippocampal part was described in detail in a previous publication (24), and we used

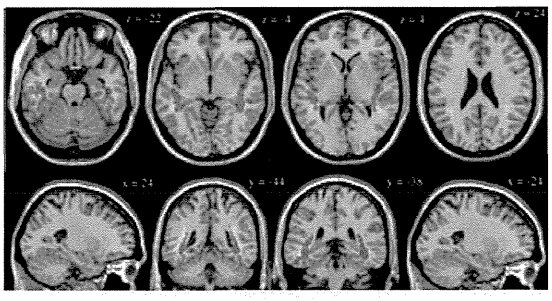

Fig. 1. Diffusion tensor tractography of three fibres. Red, yellow and green fibres represent the inferior longitudinal fasciculus, superior longitudinal fasciculus and cingulum hippocampus part, respectively.

these bilateral fibres within the temporal lobe as ROIs. Then, each six fibre tracts of 10 subjects were normalised to the standard space as mentioned above. The normalised six fibre tracts of 10 subjects were averaged respectively, and regarded as the normalised fibre ROIs. Figure 1 shows the fibre ROIs for SLF, ILF and the cingulum hippocampal part on the anatomically standard space.

Statistical analysis

Statistical analyses for the grey matter volume were performed using SPM2 software. First, we evaluate the difference among the three groups using the one-way analysis of variance (ANOVA). Only correlations that met these criteria were deemed statistically significant. In this case, seed levels of $p < 0.001$ (uncorrected) were selected. Then, the *post hoc* analysis, the differences in regional grey matter volume between first-episode schizophrenic patients and healthy subjects, high-risk groups and healthy subjects and first-episode schizophrenia and the high-risk groups were assessed using the mask image derived from the result of first-level ANOVA, respectively. Only correlations that met these criteria [seed levels of $p < 0.001$ (uncorrected), and cluster levels of $p < 0.05$ (uncorrected)] were deemed statistically significant.

Statistical analysis for the FA value was performed with SPSS for Windows 11.0 (SPSS Japan, Tokyo, Japan). Group differences of regional FA values among the three groups were compared with repeated measures of ANOVA. When significant group or group × region interactions were obtained with ANOVA, follow-up t-tests were performed for regional FA values of individual ROIs. The least significant difference method was used to avoid type 1 errors in the statistical analysis of multiplicity.

Results

There were significant volume differences in cortical volume among the two patient groups and healthy subjects. First, there were statistically volume differences in the bilateral temporal cortices between the high-risk patients and healthy subjects (Figure 2, upper column; Table 1). Second, volume losses in the bilateral temporal cortices and anterior cingulate cortex (ACC) were detected between the first-episode schizophrenia group and healthy subjects (Figure 2, lower column; Table 1). The locations of the bilateral temporal cortices detected by these analyses were almost the same coordinate (Figure 2). No differences were detected between the high-risk patients and first-episode schizophrenia patients in our study (data not shown).

The ANOVA of FA values for the healthy subjects and patient groups showed a significant main effect of group and regions. Follow-up unpaired t-tests revealed that the mean FA value of the healthy subjects was significantly higher in the bilateral SLF regions (Table 2) than in the two patient groups.

Table 1. Regions of statistically significant cerebral grey matter volume change among the three groups: one-way ANOVA among the schizophrenia, high-risk patient and healthy subject

Cluster size	T score	x	y	z	Brain region
Post hoc analysis					
Healthy subject > high-risk patient					
1024	5.20	−57	−53	−6	Left middle temporal region
730	5.45	66	−33	−9	Right middle temporal region
Healthy subject > first-episode schizophrenia					
1372	5.77	−60	−53	−7	Left middle temporal region
465	5.48	−57	−38	6	Left middle temporal region
807	5.55	66	−35	−8	Right middle temporal region
600	4.69	8	48	−7	Right anterior cingulate
	4.68	−5	48	3	Left anterior cingulate

Discussion

To the best of our knowledge, this is the first investigation of brain alterations in a clinical high-risk sample showing perceptual disturbance revealed by Rorschach test. Perceptual and thought disorders are commonly associated with psychiatric disorders and are particularly considered a primary feature of schizophrenia. Some preceding studies showed that the high-risk populations present disorders of thought, perceptual abnormalities and disorganised speech (16,17,25,26). In this study, we pointed on the perceptual disturbance as the major symptom of the high-risk patients. Furthermore, we found that there were precedent changes in the brains of high-risk patients revealed by 3D-volume data and DTI. This

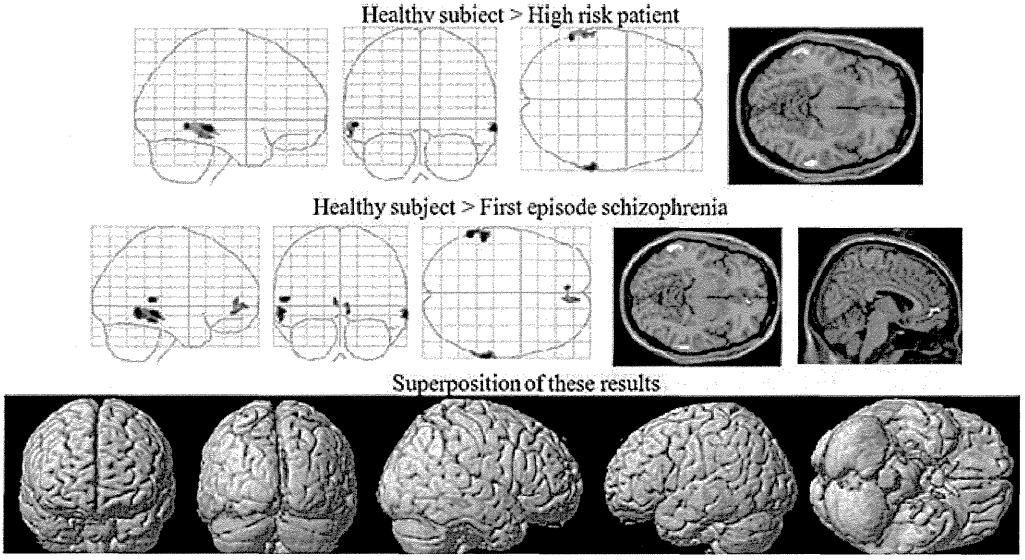

Fig. 2. Cortical grey matter volume loss was detected among the high-risk patients, first-episode schizophrenia and healthy subjects. Upper column: significant volume differences were detected in the bilateral temporal areas between the healthy subjects and high-risk patients (one-way ANOVA). Middle column: significant volume losses were detected not only in the bilateral temporal area but in the anterior cingulate cortex between the first-episode schizophrenia patients and healthy subjects. Lower column: superposition of upper two results. Yellow showed the difference between the healthy subjects and high-risk patients, green pointed the difference between the first-episode schizophrenia patients and healthy subjects and dark green showed the layered region.

Table 2. White matter DTI measurement in six fibre tracts

		FES ($N = 9$)	pre-onset patients ($N = 10$)	HS ($N = 10$)	F	df	p
LT_ILF	Mean FA	0.40 ± 0.02	0.39 ± 0.02	0.41 ± 0.02	2.75	2	0.082
	Range	0.37–0.44	0.36–0.42	0.38–0.44			
LT_CHP	Mean FA	0.25 ± 0.02	0.25 ± 0.02	0.25 ± 0.02	0.03	2	0.971
	Range	0.22–0.28	0.22–0.28	0.20–0.27			
LT_SLF	Mean FA	0.40 ± 0.02	0.38 ± 0.04	0.43 ± 0.03	5.78	2	0.008*
	Range	0.36–0.43	0.33–0.45	0.39–0.49			
RT_ILF	Mean FA	0.41 ± 0.02	0.41 ± 0.02	0.42 ± 0.02	1.29	2	0.293
	Range	0.39–0.45	0.38–0.43	0.38–0.45			
RT_CHP	Mean FA	0.26 ± 0.02	0.25 ± 0.03	0.26 ± 0.03	0.35	2	0.711
	Range	0.24–0.32	0.21–0.29	0.20–0.31			
RT_SLF	Mean FA	0.44 ± 0.02	0.44 ± 0.03	0.48 ± 0.02	10.31	2	0.001*
	Range	0.43–0.37	0.38–0.47	0.44–0.50			

Post hoc t-test

		p
LT_SLF		
HS	FES	0.048*
	Pre-onset	0.002*
FES	HS	0.048*
	Pre-onset	0.239
Pre-onset	HS	0.002*
	FES	0.239
RT_SLF		
HS	FES	0.002*
	Pre-onset	<0.001*
FES	HS	0.002*
	Pre-onset	0.430
Pre-onset	HS	<0.001*
	FES	0.430

CHP, cingulum hippocampal part; FES, first-episode schizophrenia; HS, healthy subject.
*$p > 0.05$ (correct).

should make it easier to understand the brain changes that will occur as the disease proceeds.

Some schizophrenia studies have shown left temporal impairment (27–29), while others indicate disruptions of the bilateral temporal area (30–32). In addition, a previous study showed that compared with healthy controls, high-risk subjects for schizophrenia showed lower FA in SLF (19). We observed a volume loss in the bilateral temporal cortices and microstructural disturbance in the bilateral SLF. Consistent with the findings of previous studies that used DTI, 3D-T1 weighted volume data and post-mortem brain study, the present study provides direct *in vivo* evidence of structural anomalies in patient groups. Anomalies of temporal regions have found in patients with schizophrenia, and are associates with delusions and hallucinations (33–36). Previous studies showed that the brain change preceded the episode of clinical symptoms (7–11). Our participants at high risk who did not show the delusion and hallucination may develop the precedent morphological change that would affect on the delusion and hallucination. Some neuroimaging studies focussed on the prodromal state have shown temporal lobe anomalies, but the results on the localisation of disturbance were controversial. Some studies have shown left temporal impairment using DTI and volume data (8,10). However, one study indicated reduction of the bilateral temporal grey matter (11), and some papers denied the temporal change using DTI (7,9). These inconsistencies may result from that they used intake criterion for identifying participants at high risk that included so many psychotic symptoms, such as perceptual disturbance, disorganisation, delusion, hallucination and decrease in mental state or functioning. In this study, we regarded the patients who showed perceptual disturbance revealed by the Rorschach test as the high-risk group that fell under the group 1 of the PACE criteria. By using the simple intake criterion, useful information was obtained. Furthermore, structural and functional imaging studies have revealed that the high-risk group is associated with regional volumetric and functional abnormalities that are qualitatively similar to those in patients with

schizophrenia but are less severe (37). The present observations need to be replicated with a larger study population.

In this study, our participants showed the perceptual impairment. The parietal lobe is known to be an essential part of the sensory integration (38), and it could be expected that there were morphological changes of parietal regions in high risk and schizophrenic patients. However, our results did not show the change of parietal region. Previous study that intended the early-onset schizophrenia showed the parietal abnormality (39), though the other studies unlikely show the parietal change (1,3). Previous childhood-onset schizophrenic study suggested that schizophrenic brain change in parietal lobe was obvious in youth, but the changes appear to be diminished with age (40). Our results that did not show the parietal change may be because the mean age of our participants was in the middle of 20s, and the loss of parietal lobe was attenuated.

Functional, anatomical and histopathological studies provide considerable evidence that the connections between subregions of the cingulate cortex and other brain regions are disturbed in schizophrenia (41,42). Previous neuroimaging studies have shown abnormalities of ACC in schizophrenia (43). In this study, the volume loss in ACC was detected not in the high-risk patient group but in the first-episode schizophrenia group. This may result from the fact that the schizophrenic brain shrinkage progress from posterior to anterior (44). Further follow-up studies that focus on the conversion from the prodromal state into schizophrenia are needed to reveal the pattern of ACC shrinkage.

In this study, we evaluated only a few participants. Further work with the large sample size will be necessary to confirm our results.

In summary, the present study confirms that there are proceeding changes in the brains of schizophrenic patients at the pre-onset state. The findings indicate that brain impairments may be altered in patients at the pre-onset of psychosis, possibly as a result of disrupted developmental mechanisms, and, furthermore, that these pathological changes may be predictive of functional outcome. The present observations remain to be replicated with a larger study population and with follow-up of the high-risk patients.

References

1. Shenton ME, Dickey CC, Frumin M, McCarley RW. A review of MRI findings in schizophrenia. Schizophr Res 2001;**49**:1–52.
2. Kanaan RA, Kim JS, Kaufmann WE, Pearlson GD, Barker GJ, McGuire PK. Diffusion tensor imaging in schizophrenia. Biol Psychiatry 2005;**58**:921–929.
3. Kubicki M, McCarley R, Westin CF, Park HJ, Maier S, Kikinis R. A review of diffusion tensor imaging studies in schizophrenia. J Psychiatr Res 2007;**41**:15–30.
4. Bearden CE, Rosso IM, Hollister JM, Sanchez LE, Hadley T, Cannon TD. A prospective cohort study of childhood behavioral deviance and language abnormalities as predictors of adult schizophrenia. Schizophr Bull 2000;**26**:395–410.
5. Jones P, Rodgers B, Murray R, Marmot M. Child development risk factors for adult schizophrenia in the British 1946 birth cohort. Lancet 1994;**344**:1398–1402.
6. Yung AR, Phillips LJ, McGorry PD et al. Prediction of psychosis: a step towards indicated prevention of schizophrenia. Br J Psychiatry 1998;**172**:14–20.
7. Bloemen OJ, de Koning MB, Schmitz N et al. White-matter markers for psychosis in a prospective ultra-high-risk cohort. Psychol Med 2009;**9**:1–8.
8. Borgwardt SJ, Riecher-Rössler A, Dazzan P et al. Regional gray matter volume abnormalities in the at risk mental state. Biol Psychiatry 2007;**61**:1148–1156.
9. Hoptman MJ, Nierenberg J, Bertisch HC et al. A DTI study of white matter microstructure in individuals at high genetic risk for schizophrenia. Schizophr Res 2008;**106**: 115–124.
10. Jacobson S, Kelleher I, Harley M et al. Structural and functional brain correlates of subclinical psychotic symptoms in 11-13 year old schoolchildren. Neuroimage 2010;**49**:1875–1885.
11. Job DE, Whalley HC, Johnstone EC, Lawrie SM. Grey matter changes over time in high risk subjects developing schizophrenia. Neuroimage 2005;**25**:1023–1030.
12. Exner JE Jr. A primer for Rorschach interpretation. Asheville, NC: Rorschach Workshops; 2000.
13. Exner JE Jr. 2000 alumni newsletter. Asheville, NC: Rorschach Workshops; 2000.
14. Miller TJ, McGlashan TH, Rosen JL et al. Prospective diagnosis of the initial prodrome for schizophrenia based on the structured interview of for prodromal syndromes: preliminary evidence of interrater reliability and predictive validity. Am J Psychiatry 2002;**159**:863–865.
15. Dao TK, Prevatt FA. Psychometric evaluation of the Rorschach comprehensive system's perceptual thinking index. J Pers Assess 2006;**86**:180–189.
16. Ilonen T, Heinimaa M, Korkeila J, Svirskis T, Salokangas RK. Differentiating adolescents at clinical high risk for psychosis from psychotic and non-psychotic patients with the Rorschach. Psychiatry Res 2010;**179**: 151–156.
17. Kimhy D, Corcoran C, Harkavy-Friedman JM, Ritzler B, Javitt DC, Malaspina D. Visual form perception: a comparison of individuals at high risk for psychosis, recent onset schizophrenia and chronic schizophrenia. Schizophr Res 2007;**97**:25–34.
18. Borgwardt SJ, McGuire PK, Aston J et al. Reductions in frontal, temporal and parietal volume associated with the onset of psychosis. Schizophr Res 2008;**106**:108–114.
19. Karlsgodt KH, Niendam TA, Bearden CE, Cannon TD. White matter integrity and prediction of social and role functioning in subjects at ultra-high risk for psychosis. Biol Psychiatry 2009;**66**:562–569.
20. Wakana S, Jiang H, Nagae-Poetscher LM, van Zijl PC, Mori S. Fiber tract-based atlas of human white matter anatomy. Radiology 2004;**230**:77–87.

21. Good CD, Johnsrude I, Ashburner J, Henson RNA, Friston KJ, Frackowiak RSJ. Cerebral asymmetry and the effect of sex and handedness on brain structure: a voxel-based morphometric analysis of 465 normal adult human brains. Neuroimage 2001;**14**:685–700.
22. Snook L, Plewes C, Beaulieu C. Voxel based versus region of interest analysis in diffusion tensor imaging of neurodevelopment. Neuroimage 2007;**34**:243–252.
23. Huang H, Zhang J, Jiang H, Wakana S, Poetscher L, Miller MI. DTI tractography-based parcellation of white matter: application of the mid-sagittal morphology of corpus callosum. Neuroimage 2005;**26**:295–305.
24. Wakana S, Caprihan A, Panzenboeck MM et al. Reproducibility of quantitative tractography methods applied to cerebral white matter. Neuroimage 2007;**36**:630–644.
25. McGorry PD, Yung AR, Phillips LJ. The "close-in" or ultra high-risk model: a safe and effective strategy for research and clinical intervention in prepsychotic mental disorder. Schizophr Bull 2003;**29**:771–790.
26. Pantelis C, Velakoulis D, McGorry PD et al. Neuroanatomical abnormalities before and after onset of psychosis: a cross-sectional and longitudinal MRI comparison. Lancet 2003;**361**:281–288.
27. Kasai K, Shenton ME, Salisbury DF et al. Progressive decrease of left superior temporal gyrus gray matter volume in patients with first-episode schizophrenia. Am J Psychiatry 2003;**160**:156–164.
28. Szeszko PR, Ardekani BA, Ashtari M et al. White matter abnormalities in first-episode schizophrenia or schizoaffective disorder: a diffusion tensor imaging study. Am J Psychiatry 2005;**162**:602–605.
29. van Haren NE, Hulshoff Pol HE, Schnack HG et al. Focal gray matter changes in schizophrenia across the course of the illness: a 5-year follow-up study. Neuropsychopharmacology 2007;**32**:2057–2066.
30. Andreasen NC, O'Leary DS, Flaum M et al. Hypofrontality in schizophrenia: distributed dysfunctional circuits in neuroleptic-naive patients. Lancet 1997;**349**:1730–1734.
31. Ardekani BA, Nierenberg J, Hoptman MJ, Javitt DC, Lim KO. MRI study of white matter diffusion anisotropy in schizophrenia. Neuroreport 2003;**14**:2025–2029.
32. Mathalon DH, Sullivan EV, Lim KO, Pfefferbaum A. Progressive brain volume changes and the clinical course of schizophrenia in men: a longitudinal magnetic resonance imaging study. Arch Gen Psychiatry 2001;**58**:148–157.
33. Chan WY, Yang GL, Chia MY, Lau IY, Sitoh YY, Nowinski WL, Sim K. White matter abnormalities in first-episode schizophrenia: a combined structural MRI and DTI study. Schizophr Res 2010;**119**:52–60.
34. Hubl D, Koenig T, Strik W et al. Pathways that make voices: white matter changes in auditory hallucinations. Arch Gen Psychiatry 2004;**61**:658–668.
35. Shergill SS, Kanaan RA, Chitnis XA et al. A diffusion tensor imaging study of fasciculi in schizophrenia. Am J Psychiatry 2007;**164**:467–473.
36. Yamasaki S, Yamasue H, Abe O et al. Reduced planum temporale volume and delusional behaviour in patients with schizophrenia. Eur Arch Psychiatry Clin Neurosci 2007;**257**:318–324.
37. Benetti S, Mechelli A, Picchioni M, Broome M, Williams S, McGuire P. Functional integration between the posterior hippocampus and prefrontal cortex is impaired in both first episode schizophrenia and the at risk mental state. Brain 2009;**132**:2426–2436.
38. Torrey EF. Schizophrenia and the inferior parietal lobule. Schizophr Res 2007;**97**:215–225.
39. Kyriakopoulos M, Perez-Iglesias R, Woolley JB et al. Effect of age at onset of schizophrenia on white matter abnormalities. Br J Psychiatry 2009;**195**:346–353.
40. Greenstein D, Lerch J, Shaw P et al. Childhood onset schizophrenia: cortical brain abnormalities as young adults. J Child Psychol Psychiatry 2006;**47**:1003–1012.
41. Benes FM. Neurobiological investigations in cingulate cortex of schizophrenic brain. Schizophr Bull 1993;**19**: 537–549.
42. Benes FM. Emerging principles of altered neural circuitry in schizophrenia. Brain Res Rev 2000;**31**:251–269.
43. Glahn DC, Laird AR, Ellison-Wright I et al. Meta-analysis of gray matter anomalies in schizophrenia: application of anatomic likelihood estimation and network analysis. Biol Psychiatry 2008;**64**:774–781.
44. Thompson PM, Vidal C, Giedd JN et al. Mapping adolescent brain change reveals dynamic wave of accelerated gray matter loss in very early-onset schizophrenia. Proc Natl Acad Sci U S A 2001;**98**:11650–11655.

Progress in Neuro-Psychopharmacology & Biological Psychiatry 35 (2011) 1877–1883

Contents lists available at ScienceDirect

Progress in Neuro-Psychopharmacology & Biological Psychiatry

journal homepage: www.elsevier.com/locate/pnp

A polymorphism of the *ABCA1* gene confers susceptibility to schizophrenia and related brain changes

Miho Ota [a,*,1], Takashi Fujii [a,1], Kiyotaka Nemoto [b,c], Masahiko Tatsumi [d], Yoshiya Moriguchi [c], Ryota Hashimoto [a,e,f], Noriko Sato [c], Nakao Iwata [g,h], Hiroshi Kunugi [a]

[a] *Department of Mental Disorder Research, National Institute of Neuroscience, National Center of Neurology and Psychiatry, 4-1-1 Ogawa-Higashi, Kodaira, Tokyo 187-8502, Japan*
[b] *Division of Psychiatry, Tsukuba University Hospital, 2-1-1 Amakubo, Tsukuba, Ibaraki 305-8576, Japan*
[c] *Department of Radiology, National Center of Neurology and Psychiatry, 4-1-1, Ogawa-Higashi, Kodaira, Tokyo 187-8551, Japan*
[d] *Yokohama Shinryo Clinic, Yokohama 221-0835, Japan*
[e] *Molecular Research Center for Children's Mental Development, United Graduate School of Child Development, Osaka University, Kanazawa University and Hamamatsu University School of Medicine, D3, 2-2, Yamadaoka, Suita, Osaka, 565-0871, Japan*
[f] *Department of Psychiatry, Osaka University Graduate School of Medicine, D3, 2-2, Yamadaoka, Suita, Osaka, 565-0871, Japan*
[g] *Department of Psychiatry, School of Medicine, Fujita Health University, Toyoake, Aichi, Japan*
[h] *Japan Science and Technology Agency, the Core Research for Evolutional Science and Technology, Kawaguchi, Japan*

ARTICLE INFO

Article history:
Received 14 April 2011
Received in revised form 14 July 2011
Accepted 26 July 2011
Available online 3 August 2011

Keywords:
ATP-binding cassette transporter A1
Polymorphism
Schizophrenia
Voxel based morphometry

ABSTRACT

Objective: The ATP-binding cassette transporter A1 (ABCA1) mediates cellular cholesterol efflux through the transfer of cholesterol from the inner to the outer layer of the cell membrane and regulates extracellular cholesterol levels in the central nervous system. Several lines of evidence have indicated lipid and myelin abnormalities in schizophrenia.
Method: Initially, we examined the possible association of the polymorphisms of the ABCA1 gene (*ABCA1*) with susceptibility to schizophrenia in 506 patients with schizophrenia (DSM-IV) and 941 controls. The observed association was then subject to a replication analysis in an independent sample of 511 patients and 539 controls. We further examined the possible effect of the risk allele on gray matter volume assessed with magnetic resonance imaging (MRI) in 86 patients with schizophrenia (49 males) and 139 healthy controls (47 males).
Results: In the initial association study, the 1587 *K* allele (rs2230808) was significantly more common in male patients with schizophrenia than in male controls. Although such a significant difference was not observed in the second sample alone, the increased frequency of the 1587 K allele in male patients remained to be significant in the combined male sample of 556 patients and 594 controls. Male schizophrenia patients carrying the 1587 *K* allele had a smaller amount of gray matter volume than those who did not carry the allele.
Conclusion: Our data suggest a male-specific association of the 1587 *K* allele of *ABCA1* with susceptibility to schizophrenia and smaller gray matter volume in schizophrenia.

1. Introduction

The ATP-binding cassette transporter A1 (ABCA1) mediates cellular cholesterol efflux through transfer of cholesterol from the inner to the outer layer of the cell membrane, enabling the binding of cholesterol to apolipoproteins (Knight, 2004). It plays a critical role in the regulation of extracellular cholesterol levels in the central nervous system (CNS). Mice lacking the ABCA1 gene (*ABCA1*) had significantly reduced cholesterol levels in the cerebrospinal fluid (Wahrle et al., 2004). Moreover, *ABCA1* polymorphisms are reported to be associated with serum cholesterol concentration. For instance, the 219*K* (rs2230806) allele was associated with high plasma levels of low-density lipoprotein (LDL) cholesterol (Katzov et al., 2004), and the 771*M* (rs2066718) and the 1587*K* (rs2230808) alleles were associated with low plasma levels of high-density lipoprotein (HDL) cholesterol (Clee et al., 2001; Frikke-Schmidt et al., 2004). Cholesterol is required for myelination (Saher

Abbreviations: ABCA1, ATP-binding cassette transporter A1; ANCOVA, analysis of covariance; ANOVA, analysis of variance; CNS, central nervous system; DNA, deoxyribonucleic acid; DSM-IV, Diagnostic and Statistical Manual of Mental Disorders, 4th edition; FDR, false discovery rate; FWE, familywise error rate; GWAS, genome-wide association study; HDL, high-density lipoprotein; HWE, Hardy–Weinberg equilibrium; IL1β, interleukin-1 β; LDL, low-density lipoprotein; MINI, Mini-International Neuropsychiatric Interview; MRI, magnetic resonance imaging; mRNA, messenger ribonucleic acid; PCR, polymerase chain reaction; SNP, single nucleotide polymorphisms; SPM, Statistical Parametric Mapping; TE, echo time; TR, repetition time; VBM, voxel-based morphometry

* Corresponding author. Tel.: +81 42 341 2712; fax: +81 42 346 2094.
E-mail address: ota@ncnp.go.jp (M. Ota).
[1] Contributed equally to this work.

0278-5846/$ – see front matter © 2011 Elsevier Inc. All rights reserved.
doi:10.1016/j.pnpbp.2011.07.012

et al., 2005), dendrite differentiation (Goritz et al., 2005) and synaptogenesis (Mauch et al., 2001). Therefore ABCA1 expressed in neurons and glial cells plays an important role in the regulation of synaptic development (Karasinska et al., 2009). Estrogen administration is also known to increase *ABCA1* messenger ribonucleic acid (mRNA) (Srivastava, 2002), and a sex difference in the activity of cholesterol transport has been observed (Catalano, 2008). Disturbances in CNS cholesterol homeostasis have been implicated in neurodegenerative diseases including Alzheimer's (Vance et al., 2005) and Huntington's diseases (Valenza et al., 2005). Previous studies have examined the association between polymorphisms of *ABCA1*, particularly the non-synonymous single nucleotide polymorphisms (SNPs) of rs2230806 (*R219K*), rs2066718 (*V771M*), and rs2230808 (*R1587K*) and risk for Alzheimer's disease. Some of these studies have shown a significant association (Katzov et al., 2004; Sundar et al., 2007; Shibata et al., 2006), although this association demonstrated a sex difference (Sundar et al., 2007). Several studies have demonstrated myelin abnormalities in schizophrenia (Thomas et al., 2001; Hakak et al., 2001; Garver et al., 2008; Tkachev et al., 2003; Huang and Chen, 2005), and the relationship between schizophrenia and ABCA1 was also noted (Chen et al., 2009). To date, sterol-regulatory-element binding protein-2 (SREBP-2), that regulates the ABCA1 (Wong et al., 2006), was suggested to be associated with schizophrenia (Le Hellard et al., 2010). Recent genetic studies also have revealed that the interleukin-1 β (IL1β) gene or the IL1 gene complex is associated with schizophrenia (Xu and He, 2010), and it is also suggested that change in IL1β levels in cerebrospinal fluid and serum may play a role in the pathophysiology of schizophrenia (Barak et al., 1995). IL-1β has been shown to down-regulate ABCA1 (Chen et al., 2007). However, to our knowledge, no study has thus far focused on the association between *ABCA1* polymorphisms and risk of schizophrenia. To our knowledge, no genome-wide association study (GWAS) has suggested that this chromosomal region contains a susceptibility locus for schizophrenia yet. However, some GWASs for bipolar disorder have reported this locus as a candidate region. Data from GWASs are also beginning to provide strong support for shared genetic risk across the disorders (Venken et al., 2005; Park et al., 2004; Liu et al., 2003; Badenhop et al., 2002). Interestingly, a recent study using data from GWASs strongly supported the hypothesis of shared genetic risk between schizophrenia and bipolar disorder (Moskvina et al., 2009). Thus we examined the possibility of association between the *ABCA1* variants and schizophrenia.

Previous magnetic resonance imaging (MRI) studies in schizophrenia have shown gray matter volume reduction, particularly in the insula, anterior cingulate cortex, medial frontal cortex, and hippocampal area (Fornito et al., 2009; Glahn et al., 2008). Furthermore, studies have shown the effect of disease-associated genes on such structural abnormalities in the brain (Mata et al., 2009). Deviations in brain morphology potentially reflecting genetic risk have been ubiquitous in the literature, and quantitative measures of brain structure using various neuroimaging techniques have a long history as effective endophenotype (Honea et al., 2008). In this study, we examined whether genetic variations of *ABCA1* are associated with the development of schizophrenia. We also investigated the potential influence of the disease-associated genotype of *ABCA1* on the regional cerebral gray matter volume measured with MRI.

2. Methods

2.1. Subjects

2.1.1. Initial study (Tokyo sample)

Subjects were 506 patients with schizophrenia (278 males, mean age 44.3 ± 14.1 years), diagnosed according to the Diagnostic and Statistical Manual of Mental Disorders, 4th edition (DSM-IV) (American Psychiatric Association, 1994), and 941 healthy controls (334 males, 44.8 ± 16.3 years). All patients and controls were biologically unrelated Japanese who resided in the same geographical area (the western part of Tokyo). Consensus diagnosis by at least two psychiatrists was made for each patient based on all the available information obtained from interviews and medical records. Healthy controls were interviewed for enrollment by research psychiatrists using the Japanese version of the Mini-International Neuropsychiatric Interview (MINI; Otsubo et al., 2005; Sheehan et al., 1998). Those who demonstrated no history of psychiatric illness or contact with psychiatric services were enrolled as controls in this study. Participants were excluded if they had a prior medical history of CNS disease or severe head injury. Among the subjects, 86 (49 males) schizophrenia patients and 139 healthy controls (47 males) underwent brain MRI.

2.1.2. Replication study (Tokai sample)

For the replication analysis, we used an independent Japanese sample comprising 511 cases (283 males, mean age 43.8 ± 14.9 years) and 539 controls (267 males, 36.3 ± 14.2 years). All subjects were unrelated, living in the Tokai area of the mainland of Japan, and self-identified as Japanese. Control subjects were members of the general public who had no personal history of mental disorders. This was ascertained in face-to-face interviews where subjects were asked if they had suffered an episode of depression, mania, or psychotic experiences or if they had received treatment for any psychiatric disorder. Patients were entered into the study if they 1) met DSM-IV criteria for schizophrenia; 2) were physically healthy and had normal routine laboratory tests; and 3) had no mood disorders, substance abuse, neurodevelopmental disorders, epilepsy, or known mental retardation. Consensus diagnoses were made by at least two experienced psychiatrists according to DSM-IV criteria on the basis of unstructured interviews with patients and families and review of medical records.

After description of the study, written informed consent was obtained from each subject. This study was approved by institutional ethics committees.

2.2. SNP selection and genotyping

Since genetic variations that result in an amino acid change are most likely to alter function, we searched for non-synonymous polymorphisms of *ABCA1* in the NCBI dbSNP database (http://www.ncbi.nlm.nih.gov/sites/entrez?db=snp). We also searched the literature for polymorphisms of *ABCA1* previously reported to be associated with CNS diseases. We found only four well-validated SNPs with a heterozygosity value of >0.10 in Asian populations: rs2230806 (*R219K*), rs2066718 (*V771M*), rs2066714 (*I883M*), and rs2230808 (*R1587K*). Venous blood was drawn from the subjects and genomic deoxyribonucleic acid (DNA) was extracted from whole blood according to the standard procedures. The four SNPs were genotyped using the TaqMan 5′-exonuclease allelic discrimination assay; the assay IDs were C___2741051_1_ for rs2230806, C__11720789_10 for rs2066718, C___2741083_1_ for rs2066714, and C___2741104_1_ for rs2230808 (Applied Biosystems, Foster City, CA). Thermal cycling conditions for polymerase chain reaction (PCR) were 1 cycle at 95 °C for 10 min followed by 50 cycles of 92 °C for 15 s and 60 °C for 1 min. After amplification, the allele-specific fluorescence was measured on ABI PRISM 7900 Sequence Detection (Applied Biosystems). The genotypes were scored using the software SDS2.1. Failed reactions were called as 'undetermined' by this one and these data were not included in the analysis. Genotype data were read blind to the case–control status.

2.3. MRI data acquisition and processing

All MR studies were performed on a 1.5 Tesla Siemens Magnetom Vision plus system. A three-dimensional (3D) volumetric acquisition of a T1-weighted gradient echo sequence produced a gapless series of 144 sagittal sections using an MPRAGE sequence (echo time (TE)/repetition time (TR): 4.4/11.4 ms; flip angle: 15°; acquisition

matrix: 256×256; 1NEX, field of view: 31.5 cm; slice thickness: 1.23 mm). The raw 3D T1-weighted volume data were transferred to a workstation, and structural images were analyzed using an optimized, voxel-based morphometry (VBM) technique. Data were analyzed using Statistical Parametric Mapping 5 (SPM5) software (Welcome Department of Imaging Neuroscience, London, UK) running on MATLAB 7.0 (Math Works, Natick, MA). Images were processed using an optimized VBM script. The details of this process are described elsewhere (Li and Ji, 2005). First, each individual 3D-T1 image was normalized with the optimized VBM method. Normalized segmented images were modulated by multiplication with Jacobian determinants of the spatial normalization function to encode the deformation field for each subject as tissue density changes in normal space. Images were smoothed using an 8-mm full-width at half-maximum of an isotropic Gaussian kernel.

2.4. Statistical analysis

Deviations of genotype distributions from the Hardy–Weinberg equilibrium (HWE) were assessed with the χ^2 test for goodness of fit. First, genotype distributions were compared between patients and controls using the χ^2 test for independence. Since some animal studies showed the gender specific findings (Koldamova et al., 2005; Kuivenhoven et al., 2003), and estrogen has functional relevance to the *ABCA1*-mediated pathway (Srivastava, 2002) and a sex difference in the activity of cholesterol transport has been observed (Catalano et al., 2008), analysis for each sex was also performed. These tests were performed with SPSS software ver. 11 (SPSS Japan, Tokyo, Japan). For multiple analyses, we applied the spectral decomposition method of SNPSpD software (http://gump.qimr.edu.au/general/daleN/SNPSpD/) (Nyholt, 2004; Li and Ji, 2005), which considers marker linkage disequilibrium information and generates an experiment-wide significance threshold required to keep the type I error rate at 5%. As a result, the critical P value was corrected as 0.0128. Then, the observed association was subject to a replication analysis in an independent Tokai sample using the χ^2 test for independence.

Second, we then evaluated the differences in regional gray matter volume across the clusters sorted by the genotype distributions of the SNP that showed a statistically significant difference between the patients and healthy subjects. Statistical analyses were performed using Statistical Parametric Mapping 2 (SPM2) software (Welcome Department of Imaging Neuroscience, London, UK). Since the regional cerebral gray matter volume is influenced by age (Good et al., 2001), we examined the differences in regional gray matter volume by the analysis of covariance (ANCOVA), controlling for age. Only associations that met the following criteria were deemed statistically significant for the first analysis: familywise error rate (FWE)<0.05, and for the *post hoc* analyses: a voxel level of $p<0.001$ (uncorrected) and a cluster level of $p<0.05$ (uncorrected). We also evaluated the differences across the groups according to age using one-way analysis of variance (ANOVA) and the differences between two groups of schizophrenia patients categorized according to duration of illness and daily dose of antipsychotic drugs using a two-sample *t*-test.

3. Results

3.1. ABCA1 polymorphisms and susceptibility to schizophrenia

First, genotype and allele distributions of the 4 SNPs in the initial sample (Tokyo sample) are shown in Table 1. The genotype distribution for rs2230806 in the female control group deviated significantly from the HWE, thus was excluded from further analysis. In the total sample, the genotype or allele distribution did not differ significantly between the cases and controls for any SNP. However, when men and women were examined separately, a nominally significant difference in the genotype distribution for rs2230808 (*R1587K*) was observed in men ($p=0.014$), but not in women ($p=0.674$). Difference in allele frequency was observed at a trend level in men ($p=0.055$), but not in women ($p=0.440$). When the observed difference in the genotype distribution for rs2230808 was further analyzed based on the recessive and dominant models, there was a significant difference in the dominant model ($p=0.006$; odds ratio (OR) 1.60, 95% confidential interval (CI): 1.14–2.24), but not in the recessive one ($p=0.96$), in male subjects. There was no significant difference in genotype or allele distribution of the other 3SNPs even when subjects were stratified by sex.

Table 2 shows genotype and allele distributions for rs2230808 in the replication sample (Tokai sample). There was no significant difference in genotype or allele distribution between the patients and controls. When men and women were examined separately, there was no significant difference for either sex. We also analyzed based on the dominant model; however, no statistically significant differences in genotype distribution were found in total subjects or each sex. However, the initial and replication samples were combined, the frequency of male patients carrying the 1587K allele remained to be increased than male controls at nominally significant level (OR 1.30, 95% CI 1.02 –1.65, $p=0.032$).

3.2. ABCA1 polymorphism and MRI volumetry

Since carrying the 1587*K* allele was found to be significantly more common in male patients with schizophrenia than in male controls in the genetic association study, the subjects with MRI data were grouped into four groups for each sex based on the case–control status and whether the subject carried the 1587*K* allele or not. The demographic and clinical characteristics of the groups are presented in Table 3. For both men and women, the analyses showed no significant difference in duration of illness or daily dose of antipsychotics between the two genotype-based groups of patients with schizophrenia (men: duration of illness: $t(47)=-0.15$, $p=0.88$, daily dose of drug: $t(47)=-1.58$, $p=0.12$; female: duration of illness: $t(34)=-0.40$, $p=0.69$, daily dose of drug: $t(34)=-0.20$, $p=0.85$). Further, for both men and women, there was no significant difference in mean age across the healthy subjects and two schizophrenia groups (men: $df=2$, $F=1.54$, $p=0.22$; women: $df=2$, $F=1.16$, $p=0.32$).

Initially, we evaluated the difference in gray matter volume between the two genotype-based healthy groups for each sex using ANCOVA, controlling for age. There were no significant differences related to genotype for either sex, respectively. We therefore combined the healthy groups with and without the 1587*K* allele for each sex in the following analyses. When the group effect was assessed using ANCOVA with F-test (FWE<0.05), we found statistically significant volume differences in thalami, medial temporal regions, and nearly all the circumferential cortical regions in males (Fig. 1A). Male patients with schizophrenia carrying the 1587*K* allele showed significant small gray matter volume in the bilateral occipital regions and posterior cingulate cortices compared with those who did not carry the 1587*K* allele (Fig. 1B). Male patients with schizophrenia who did not carry the 1587*K* allele showed significant small volume only in bilateral orbitofrontal, insulae, and left parahippocampus, compared with all male controls (Fig. 1C). However, the male schizophrenia patients carrying the 1587*K* allele showed smaller volume across almost the whole gray matter, than all male controls (Fig. 1D). When we re-analyzed these *post hoc* statistics using rigorous criteria (false discovery rate (FDR) $p<0.05$, cluster level of $p<0.05$), results indicated with Fig. 1C and D showed almost the same as the previous ones, the statistics using the relatively small sample size indicated with the Fig. 1B showed no statistically significant difference between the schizophrenic groups.

In women, in contrast, there were no significant differences in gray matter volume between schizophrenia patients with and without the 1587*K* allele or between controls with and without the allele (data not

Table 1
Genotype and allelic distributions of the ABCA1 SNPs in patients with schizophrenia and controls.

db SNP ID and aminoacid change	Position*	Inter-SNP distance (bp)	Gender	Group	N	Genotype distribution (frequency)			$\chi 2$	P	Allele count (frequency)				$\chi 2$	P	HWE of Controls (df = 1)
						R/R	*R/K*	*K/K*			*R*		*K*				
rs2230806 Arg219Lys	107620867 exon 7	(-)	All	Schizophrenia	497	119 (0.24)	241 (0.48)	137 (0.28)	2.77	0.250	479	(0.48)	515	(0.52)	0.01	0.897	$\chi^2 = 3.73$
				Controls	932	204 (0.22)	495 (0.53)	233 (0.25)			903	(0.48)	961	(0.52)			P = 0.053
			M	Schizophrenia	274	63 (0.23)	137 (0.50)	74 (0.27)	0.47	0.789	263	(0.48)	285	(0.52)	0.45	0.503	$\chi^2 = 0.05$
				Controls	330	71 (0.22)	162 (0.49)	97 (0.29)			304	(0.46)	356	(0.54)			P = 0.827
			F	Schizophrenia	223	56 (0.25)	104 (0.47)	63 (0.28)			216	(0.48)	230	(0.52)			$\chi^2 = 6.81$
				Controls	602	133 (0.22)	333 (0.55)	136 (0.23)			599	(0.50)	605	(0.50)			P = 0.009
						V/V	*V/M*	*M/M*			*V*		*M*				
rs2066718 Val771Met	107589255 exon 16	31,612	All	Schizophrenia	494	438 (0.89)	54 (0.11)	2 (0.00)	1.09	0.580	930	(0.94)	58	(0.06)	0.99	0.319	$\chi^2 = 0.04$
				Controls	936	812 (0.87)	120 (0.13)	4 (0.00)			1744	(0.93)	128	(0.07)			P = 0.847
			M	Schizophrenia	273	242 (0.89)	29 (0.11)	2 (0.01)	1.70	0.428	513	(0.94)	33	(0.06)	0.50	0.480	$\chi^2 = 0.30$
				Controls	333	287 (0.86)	45 (0.14)	1 (0.00)			619	(0.93)	47	(0.07)			P = 0.582
			F	Schizophrenia	221	196 (0.89)	25 (0.11)	0 (0.00)	1.32	0.518	417	(0.94)	25	(0.06)	0.60	0.437	$\chi^2 = 0.03$
				Controls	603	525 (0.87)	75 (0.12)	3 (0.00)			1125	(0.93)	81	(0.07)			P = 0.856
						I/I	*I/M*	*M/M*			*I*		*M*				
rs2066714 Ile883Met	107586753 exon 18	34,114	All	Schizophrenia	487	208 (0.43)	212 (0.44)	67 (0.14)	3.86	0.145	628	(0.64)	346	(0.36)	1.75	0.186	$\chi^2 = 0.91$
				Controls	917	345 (0.38)	446 (0.49)	126 (0.14)			1136	(0.62)	698	(0.38)			P = 0.339
			M	Schizophrenia	266	115 (0.43)	116 (0.44)	35 (0.13)	3.23	0.199	346	(0.65)	186	(0.35)	0.87	0.335	$\chi^2 = 2.40$
				Controls	330	122 (0.37)	168 (0.51)	40 (0.12)			412	(0.62)	248	(0.38)			P = 0.122
			F	Schizophrenia	221	93 (0.42)	96 (0.43)	32 (0.14)	1.23	0.542	282	(0.64)	160	(0.36)	0.62	0.430	$\chi^2 = 0.002$
				Controls	587	223 (0.38)	278 (0.47)	86 (0.15)			724	(0.62)	450	(0.38)			P = 0.966
						R/R	*R/K*	*K/K*			*R*		*K*				
rs2230808 Arg1587Lys	107562804 exon 35	58,063	All	Schizophrenia	491	174 (0.35)	252 (0.51)	65 (0.13)	4.05	0.132	600	(0.61)	382	(0.39)	0.63	0.427	$\chi^2 = 0.50$
				Controls	923	367 (0.40)	422 (0.46)	134 (0.15)			1156	(0.63)	690	(0.37)			P = 0.478
			M	Schizophrenia	273	87 (0.32)	148 (0.54)	38 (0.14)	8.51	0.014	322	(0.59)	224	(0.41)	3.68	0.055	$\chi^2 = 1.17$
				Controls	327	140 (0.43)	141 (0.43)	46 (0.14)			421	(0.64)	233	(0.36)			P = 0.278
			F	Schizophrenia	218	87 (0.40)	104 (0.48)	27 (0.12)	0.79	0.674	278	(0.64)	158	(0.36)	0.60	0.440	$\chi^2 = 0.01$
				Controls	596	227 (0.38)	281 (0.47)	88 (0.15)			735	(0.62)	457	(0.38)			P = 0.945

HWE; Hardy–Weinberg equilibrium.
* Chromosome position was determined from the dbSNP database.

Table 2
Genotype and allelic distributions of rs2230808 in independent replication sample.

db SNP ID and aminoacid change	Gender	Group	N	Genotype distribution (frequency)			$\chi 2$	P	Allele count (frequency)				$\chi 2$	P	HWE of controls (df = 1)
				R/R	*R/K*	*K/K*			*R*		*K*				
rs2230808 Arg1587Lys	All	Schizophrenia	539	211 (0.39)	252 (0.47)	76 (0.14)	0.25	0.88	676	(0.63)	404	(0.37)	0.03	0.85	$\chi^2 = 0.49$
		Controls	511	201 (0.39)	233 (0.46)	77 (0.15)			635	(0.62)	387	(0.38)			P = 0.48
	M	Schizophrenia	283	109 (0.39)	133 (0.47)	41 (0.14)	0.15	0.93	351	(0.62)	215	(0.38)	0.14	0.71	$\chi^2 = 0.01$
		Controls	267	106 (0.40)	125 (0.47)	36 (0.13)			337	(0.63)	197	(0.37)			P = 0.92
	F	Schizophrenia	256	102 (0.40)	119 (0.46)	35 (0.14)	0.97	0.62	323	(0.63)	189	(0.37)	0.43	0.51	$\chi^2 = 1.17$
		Controls	244	95 (0.39)	108 (0.44)	41 (0.17)			298	(0.61)	190	(0.39)			P = 0.28

HWE; Hardy–Weinberg equilibrium.

shown). We evaluated the difference between the all controls and all cases using ANCOVA. The female schizophrenia patients showed smaller gray matter volume in the bilateral insulae, anterior cingulate cortex, and orbitofrontal cortex, than all female controls (Fig. 1E).

We also we evaluated the difference in gray matter volume between the schizophrenic groups with and without the 1587*K* allele for each sex using ANCOVA, controlling for age, duration of illness, educational period, and medication. There were no statistically significant differences between the groups for each sex, however, male patients with schizophrenia carrying the 1587*K* allele showed small gray matter volume in the left occipital region and bilateral posterior cingulate cortices, almost the same as Figure (B), compared with those who did not carry the 1587*K* allele at nominal trend level (F) ($P<0.01$ uncorrected). There were no differences between the female schizophrenic patients with or without the 1587*K* allele using loose criteria ($P<0.01$ uncorrected, data not shown).

4. Discussion

We found that the 1587*K* allele of *ABCA1* was significantly more common in male patients with schizophrenia than in male controls. However, such a difference was not observed in women. Furthermore, our results showed that male schizophrenic patients who carried the 1587*K* allele have smaller gray matter volume than in those who did not, but this difference did not extend to women. To our knowledge, this is the first study that reports the possible association of *ABCA1* with susceptibility to schizophrenia and related brain abnormalities.

4.1. ABCA1 polymorphisms and susceptibility to schizophrenia

The 1587*K* allele was reported to increase cerebrospinal fluid tau level and brain amyloid beta load (Katzov et al., 2004). It was also associated with low plasma levels of apolipoprotein A1 (Tregouet et al., 2004) and HDL-cholesterol (Clee et al., 2001; Frikke-Schmidt et al., 2004), suggesting functional differences between the *R*1587 and 1587*K* alleles, which may explain our results.

The present study showed gender-specific association between *R*1587*K* (rs2230808) and schizophrenia in our population. Serum from men displays an enhanced free cholesterol efflux capacity via the ABCA1 transporter pathway compared with that from perimenopausal women (Catalano et al., 2008). Estradiol was known to modulate a wide range of functions of the brain. From the onset of menopause, declining levels of estradiol can cause cognitive disturbances and changes in behavior that can be counterbalanced by hormone replacement. Studies in mice have suggested that the atheroprotective effects of estrogen may occur partly via the ABCA1-mediated pathway (Srivastava, 2002). Another study found that ABCA1 was up-regulated by estradiol (Sárvári et al., 2010). Taking these previous findings into consideration, the observed sex difference in our study may be explained, at least in part, by the fact that estrogen is involved in the regulation of ABCA1 activity. The role of CNS cholesterol in synaptic function and neurodegenerative disorders has recently been appreciated, but the mechanisms regulating its transport and homeostasis are only partially understood. Therefore, further studies that focused on the sex difference should be needed to reveal the function of the ABCA1.

In the initial study, the 1587*K* allele (rs2230808) was significantly more common in male patients with schizophrenia than in male controls. Although such a significant difference was not observed in the second sample alone, the increased frequency of the 1587K allele in male patients remained to be significant in the combined male sample. Though there was the association of *ABCA1* with susceptibility to schizophrenia, it is suggested that this relationship may be fairly weak.

4.2. ABCA1 polymorphism and MRI volumetry

Our results showed that male schizophrenia patients carrying the 1587*K* allele showed smaller gray matter volume than those who did not carry the allele. Schizophrenia has been associated with volume reductions in the limbic, paralimbic, frontal, and temporal cortical regions (Glahn et al., 2008; Ellison-Wright et al., 2008; Shenton et al., 2001; Wright et al., 2000), although some previous studies did not detect disturbances in such regions (Kanaan et al., 2005; Kubicki et al.,

Table 3
Characteristics of the subjects who underwent MRI.

		Genotype distribution of rs2230808	N	Age	Duration of illness	Drug dose (chlorpromazine equivalent)
Men	Control	*R/R*	21	39.8 ± 12.4 (20–71)		
		K carrier	26	38.9 ± 11.9 (25–69)		
		All	47	39.3 ± 12.0 (20–71)		
	Schizophrenia	*R/R*	16	44.7 ± 16.7 (22–76)	21.0 ± 16.9	770.0 ± 636.0
		K carrier	33	43.7 ± 13.0 (27–72)	21.7 ± 12.9	1183.6 ± 945.7
Women	Control	*R/R*	39	48.2 ± 13.5 (25–74)		
		K carrier	53	39.9 ± 11.6 (22–71)		
		All	92	43.4 ± 13.0 (22–74)		
	Schizophrenia	*R/R*	16	47.5 ± 12.3 (22–67)	17.2 ± 13.2	691.6 ± 566.3
		K carrier	21	46.3 ± 15.0 (23–75)	19.0 ± 13.2	731.2 ± 623.9

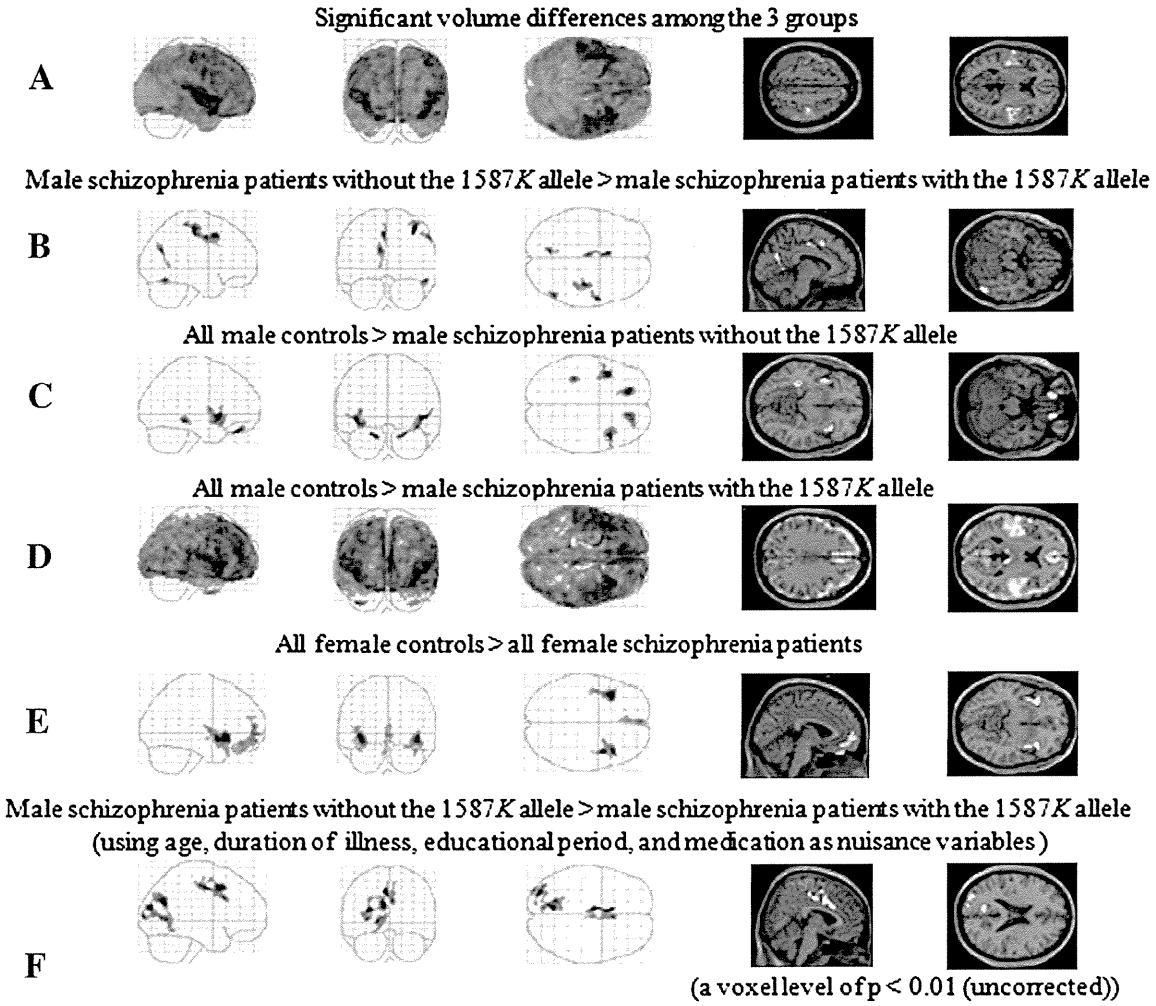

Fig. 1. Group effect was assessed using analysis of covariance (ANCOVA) (SPM2). Age was used as a nuisance variable. (A); There were statistically significant volume differences among the 3 groups of men, i.e., the male schizophrenia patients with and without the 1587*K* allele and the entire male control group. (B); Male schizophrenia patients carrying the 1587*K* allele showed gray matter volume reduction in the bilateral occipital regions and posterior cingulate cortices compared with those who did not carry this allele. (C); There were volume decreases in the bilateral insulae and orbitofrontal regions, and the left parahippocampal region in male patients with schizophrenia without the 1587*K* allele compared with all male controls. (D); Male patients with schizophrenia carrying the 1587*K* allele showed volume reduction in almost all the gray matter areas, compared with all male controls. (E); When all female schizophrenia patients were analyzed collectively, they showed gray matter volume reduction in the bilateral insulae, anterior cingulate cortex, and orbitofrontal cortex, compared with all female controls. (F); We also evaluated the difference in gray matter volume between the schizophrenic groups with and without the 1587*K* allele for each sex using ANCOVA, controlling for age, duration of illness, educational period, and medication. Male patients with schizophrenia carrying the 1587*K* allele showed small gray matter volume in the left occipital region and bilateral posterior cingulate cortices, compared with those who did not carry the 1587*K* allele controlling for age, duration of illness, educational period, and medication, at nominal trend level ($P<0.01$ uncorrected).

2007). Two broad theories have been proposed to describe the pattern of cerebral changes: the global and macro-circuit theories (Buchsbaum et al., 2006). According to the global theory, white matter reductions occur uniformly throughout the brain, possibly as a result of genetic abnormalities in the protein pathways controlling myelination (Konrad and Winterer, 2008). The alternative macro-circuit theory proposes that specific white matter tracts are disrupted in schizophrenia either as a cause or a consequence of a disorder in the gray matter regions they connect (Konrad and Winterer, 2008). The present results may accord with the global theory by showing smaller volume in almost the entire gray matter in male schizophrenia patients carrying the 1587*K* allele of *ABCA1*, because ABCA1 was regarded as the key regulator of brain cholesterol homeostasis and associated with structure and function in neurons such as myelination (Karasinska et al., 2009). Both male and female schizophrenia patients who did not carry the 1587*K* allele showed smaller volume in the medial temporal region, insulae, and anterior cingulate cortex, which have been referred to as predominantly impaired brain regions in schizophrenia, than control subjects (Glahn et al., 2008; Ellison-Wright et al., 2008). On the other hand, the male patients with schizophrenia carrying the 1587*K* allele showed the smaller volume in the occipital regions and posterior cingulate cortices, where it is known to remain unchanged from illness, than male patients not carrying 1587*K* allele. Intricate analysis controlling for age, duration of illness, educational period, and medication, male patients carrying 1587*K* allele showed the smaller volume in occipital and posterior cingulate cortices compared with male patients not carrying 1587*K* allele, only at the trend level, but these tendencies could not be detected in females even at the trend level. From these points, we suggest a male-specific association of the 1587*K* allele of *ABCA1* with susceptibility to schizophrenia and smaller gray matter volume in schizophrenia. In this study, we evaluated only a gray matter volume change, and no consideration was paid to the white matter. Further work with the diffusion tensor imaging data will be necessary to confirm our results.

Schizophrenia is a multifactorial disorder caused by a complex interaction of genetic and environmental factors (Bassett et al., 2001).

In this study, we found no significant difference in gray matter volume related to the *R1587K* polymorphism in healthy subjects. This may be accounted for by the possibility that *ABCA1* polymorphism interacts with other risk factors for schizophrenia and that these collectively influence brain vulnerability.

References

American Psychiatric Association. Diagnostic and Statistical Manual of Mental Disorders. 4th ed. Washington, DC: American Psychiatric Press; 1994.

Badenhop RF, Moses MJ, Scimone A, Mitchell PB, Ewen-White KR, Rosso A, et al. A genome screen of 13 bipolar affective disorder pedigrees provides evidence for susceptibility loci on chromosome 3 as well as chromosomes 9, 13 and 19. Mol Psychiatry 2002;7:851–9.

Barak V, Barak Y, Levine J, Nisman B, Roisman I. Changes in interleukin-1 beta and soluble interleukin-2 receptor levels in CSF and serum of schizophrenic patients. J Basic Clin Physiol Pharmacol 1995;6:61–9.

Bassett AS, Chow EW, O'Neill S, Brzustowicz LM. Genetic insights into the neurodevelopmental hypothesis of schizophrenia. Schizophr Bull 2001;27:417–30.

Buchsbaum MS, Schoenknecht P, Torosjan Y, Newmark R, Chu KW, Mitelman S, et al. Diffusion tensor imaging of frontal lobe white matter tracts in schizophrenia. Ann Gen Psychiatry 2006;5:19.

Catalano G, Duchene E, Le Julia Z, Goff W, Bruckert E, Chapman MJ, et al. Cellular SR-BI and ABCA1-mediated cholesterol efflux are gender-specific in healthy subjects. J Lipid Res 2008;49:635–43.

Chen M, Li W, Wang N, Zhu Y, Wang X. ROS and NF-kappaB but not LXR mediate IL-1beta signaling for the downregulation of ATP-binding cassette transporter A1. Am J Physiol Cell Physiol 2007;292:1493–501.

Chen X, Sun C, Chen Q, O'Neill FA, Walsh D, Fanous AH, et al. Apoptotic engulfment pathway and schizophrenia. PLoS One 2009;4:e6875.

Clee SM, Zwinderman AH, Engert JC, Zwarts KY, Molhuizen HO, Roomp K, et al. Common genetic variation in ABCA1 is associated with altered lipoprotein levels and a modified risk for coronary artery disease. Circulation 2001;103:1198–205.

Ellison-Wright I, Glahn DC, Laird AR, Thelen SM, Bullmore E. The Anatomy of first-episode and chronic schizophrenia: an anatomical likelihood estimation meta-analysis. Am J Psychiatry 2008;165:1015–23.

Fornito A, Yücel M, Patti J, Wood SJ, Pantelis C. Mapping grey matter reductions in schizophrenia: an anatomical likelihood estimation analysis of voxel-based morphometry studies. Schizophr Res 2009;108:104–13.

Frikke-Schmidt R, Nordestgaard BG, Jensen GB, Tybjaerg-Hansen A. Genetic variation in ABC transporter A1 contributes to HDL cholesterol in the general population. J Clin Invest 2004;114:1343–53.

Garver DL, Holcomb JA, Christensen JD. Compromised myelin integrity during psychosis with repair during remission in drug-responding schizophrenia. Int J Neuropsychopharmacol 2008;11:49–61.

Glahn DC, Laird AR, Ellison-Wright I, Thelen SM, Robinson JL, Lancaster JL, et al. Meta-analysis of gray matter anomalies in schizophrenia: application of anatomic likelihood estimation and network analysis. Biol Psychiatry 2008;64:774–81.

Good CD, Johnsrude I, Ashburner J, Henson RNA, Friston KJ, Frackowiak RSJ. Cerebral asymmetry and the effect of sex and handedness on brain structure: a voxel-based morphometric analysis of 465 normal adult human brains. Neuroimage 2001;14:685–700.

Goritz C, Mauch DH, Pfrieger FW. Multiple mechanisms mediate cholesterol-induced synaptogenesis in a CNS neuron. Mol Cell Neurosci 2005;29:190–201.

Hakak Y, Walker JR, Li C, Wong WH, Davis KL, Buxbaum JD, et al. Genome-wide expression analysis reveals dysregulation of myelination-related genes in chronic schizophrenia. Proc Natl Acad Sci USA 2001;98:4746–51.

Honea RA, Meyer-Lindenberg A, Hobbs KB, Pezawas L, Mattay VS, Egan MF, et al. Is gray matter volume an intermediate phenotype for schizophrenia? A voxel-based morphometry study of patients with schizophrenia and their healthy siblings. Biol Psychiatry 2008;63:465–74.

Huang TL, Chen JF. Serum lipid profiles and schizophrenia: effects of conventional or atypical antipsychotic drugs in Taiwan. Schizophr Res 2005;80:55–9.

Kanaan RA, Kim JS, Kaufmann WE, Pearlson GD, Barker GJ, McGuire PK. Diffusion tensor imaging in schizophrenia. Biol Psychiatry 2005;58:921–9.

Karasinska JM, Rinninger F, Lütjohann D, Ruddle P, Franciosi S, Kruit JK, et al. Specific loss of brain ABCA1 increases brain cholesterol uptake and influences neuronal structure and function. J Neurosci 2009;29:3579–89.

Katzov H, Chalmers K, Palmgren J, Andreasen N, Johansson B, Cairns NJ, et al. Genetic variants of ABCA1 modify Alzheimer disease risk and quantitative traits related to beta-amyloid metabolism. Hum Mutat 2004;23:358–67.

Knight BL. ATP-binding cassette transporter A1: regulation of cholesterol efflux. Biochem Soc Trans 2004;32:124–7.

Koldamova R, Staufenbiel M, Lefterov I. Lack of ABCA1 considerably decreases brainAPOElevel and increases amyloid deposition in APP23 mice. J Biol Chem 2005;280:43224–35.

Konrad A, Winterer G. Disturbed structural connectivity in schizophrenia primary factor in pathology or epiphenomenon? Schizophr Bull 2008;34:72–92.

Kubicki M, McCarley R, Westin CF, Park HJ, Maier S, Kikinis R, et al. A review of diffusion tensor imaging studies in schizophrenia. J Psychiatr Res 2007;41:15–30.

Kuivenhoven JA, Hovingh GK, van Tol A, Jauhiainen M, Ehnholm C, Fruchart JC, et al. Heterozygosity for ABCA1 gene mutations: effects on enzymes, apolipoproteins and lipoprotein particle size. Atherosclerosis 2003;171:311–9.

Le Hellard S, Mühleisen TW, Djurovic S, Fernø J, Ouriaghi Z, Mattheisen M, et al. Polymorphisms in SREBF1 and SREBF2, two antipsychotic-activated transcription factors controlling cellular lipogenesis, are associated with schizophrenia in German and Scandinavian samples. Mol Psychiatry 2010;15:463–72.

Li J, Ji L. Adjusting multiple testing in multilocus analyses using the eigenvalues of a correlation matrix. Heredity 2005;95:221–7.

Liu J, Juo SH, Dewan A, Grunn A, Tong X, Brito M, et al. Evidence for a putative bipolar disorder locus on 2p13-16 and other potential loci on 4q31, 7q34, 8q13, 9q31, 10q21-24, 13q32, 14q21 and 17q11-12. Mol Psychiatry 2003;8:333–42.

Mata I, Perez-Iglesias R, Roiz-Santiañez R, Tordesillas-Gutierrez D, Gonzalez-Mandly A, Vazquez-Barquero JL, et al. A neuregulin 1 variant is associated with increased lateral ventricle volume in patients with first-episode schizophrenia. Biol Psychiatry 2009;65:535–40.

Mauch DH, Nagler K, Schumacher S, Goritz C, Muller EC, Otto A, et al. CNS synaptogenesis promoted by glia-derived cholesterol. Science 2001;294:1354–7.

Moskvina V, Craddock N, Holmans P, Nikolov I, Pahwa JS, Green E. Welcome Trust Case Control Consortium, Owen MJ, O'Donovan MC. Gene-wide analyses of genome-wide association data sets: evidence for multiple common risk alleles for schizophrenia and bipolar disorder and for overlap in genetic risk. Mol Psychiatry 2009;14:252–60.

Nyholt DR. A simple correction for multiple testing for single-nucleotide polymorphisms in linkage disequilibrium with each other. Am J Hum Genet 2004;74:765–9.

Otsubo T, Tanaka K, Koda R, Shinoda J, Sano N, Tanaka S, et al. Reliability and validity of Japanese version of the Mini-International Neuropsychiatric Interview. Psychiatry Clin Neurosci 2005;59:517–26.

Park N, Juo SH, Cheng R, Liu J, Loth JE, Lilliston B, et al. Linkage analysis of psychosis in bipolar pedigrees suggests novel putative loci for bipolar disorder and shared susceptibility with schizophrenia. Mol Psychiatry 2004;9:1091–9.

Saher G, Brugger B, Lappe-Siefke C, Mobius W, Tozawa R, Wehr MC, et al. High cholesterol level is essential for myelin membrane growth. Nat Neurosci 2005;8:468–75.

Sárvári M, Kalló I, Hrabovszky E, Solymosi N, Tóth K, Likó I, et al. Estradiol replacement alters expression of genes related to neurotransmission and immune surveillance in the frontal cortex of middle-aged, ovariectomized rats. Endocrinology 2010;151:3847–62.

Sheehan DV, Lecrubier Y, Sheehan KH, Amorim P, Janavs J, Weiller E, et al. The Mini-International Neuropsychiatric Interview (M.I.N.I.): the development and validation of a structured diagnostic psychiatric interview for DSM-IV and ICD-10. J Clin Psychiatry 1998;59(suppl. 20):22–57.

Shenton ME, Dickey CC, Frumin M, McCarley RW. A review of MRI findings in schizophrenia. Schizophr Res 2001;49:1–52.

Shibata N, Kawarai T, Lee JH, Lee HS, Shibata E, Sato C, et al. Association studies of cholesterol metabolism genes (CH25H, ABCA1 and CH24H) in Alzheimer's disease. Neurosci Lett 2006;391:142–6.

Srivastava RA. Estrogen-induced regulation of the ATP-binding cassette transporter A1 (ABCA1) in mice: a possible mechanism of atheroprotection by estrogen. Mol Cell Biochem 2002;240:67–73.

Sundar PD, Feingold E, Minster RL, DeKosky ST, Kamboh MI. Gender-specific association of ATP-binding cassette transporter 1 (ABCA1) polymorphisms with the risk of late-onset Alzheimer's disease. Neurobiol Aging 2007;28:856–62.

Thomas EA, Dean B, Pavey G, Sutcliffe JG. Increased CNS levels of apolipoprotein D in schizophrenic and bipolar subjects: implications for the pathophysiology of psychiatric disorders. Proc Natl Acad Sci USA 2001;98:4066–71.

Tkachev D, Mimmack ML, Ryan MM, Wayland M, Freeman T, Jones PB, et al. Oligodendrocyte dysfunction in schizophrenia and bipolar disorder. Lancet 2003;362:798–805.

Tregouet DA, Ricard S, Nicaud V, Arnould I, Soubigou S, Rosier M, et al. In-depth haplotype analysis of ABCA1 gene polymorphisms in relation to plasma ApoA1 levels and myocardial infarction. Arterioscler Thromb Vasc Biol 2004;24:775–81.

Valenza M, Rigamonti D, Goffredo D, Zuccato C, Fenu S, Jamot L, et al. Dysfunction of the cholesterol biosynthetic pathway in Huntington's disease. J Neurosci 2005;25:9932–9.

Vance JE, Hayashi H, Karten B. Cholesterol homeostasis in neurons and glial cells. Semin Cell Dev Biol 2005;16:193–212.

Venken T, Claes S, Sluijs S, Paterson AD, van Duijn C, Adolfsson R, et al. Genomewide scan for affective disorder susceptibility Loci in families of a northern Swedish isolated population. Am J Hum Genet 2005;76:237–48.

Wahrle SE, Jiang H, Parsadanian M, Legleiter J, Han X, Fryer JD, et al. ABCA1 is required for normal central nervous system ApoE levels and for lipidation of astrocyte-secreted apoE. J Biol Chem 2004;279:40987–93.

Wong J, Quinn CM, Brown AJ. SREBP-2 positively regulates transcription of the cholesterol efflux gene, ABCA1, by generating oxysterol ligands for LXR. Biochem J 2006;400:485–91.

Wright IC, Rabe-Hesketh S, Woodruff PWR, David AS, Murray RM, Bullmore ET. Meta-analysis of regional brain volumes in schizophrenia. Am J Psychiatry 2000;157:16–25.

Xu M, He L. Convergent evidence shows a positive association of interleukin-1 gene complex locus with susceptibility to schizophrenia in the Caucasian population. Schizophr Res 2010;120:131–42.

Magnetic Resonance Imaging 31 (2013) 990–995

Contents lists available at SciVerse ScienceDirect

Magnetic Resonance Imaging

journal homepage: www.mrijournal.com

Abnormalities of cerebral blood flow in multiple sclerosis: A pseudocontinuous arterial spin labeling MRI study☆

Miho Ota [a,*], Noriko Sato [b], Yasuhiro Nakata [b], Kimiteru Ito [b], Kouhei Kamiya [b], Norihide Maikusa [c], Masafumi Ogawa [d], Tomoko Okamoto [d], Satoko Obu [a], Takamasa Noda [e], Manabu Araki [d], Takashi Yamamura [f], Hiroshi Kunugi [a]

[a] Department of Mental Disorder Research, National Institute of Neuroscience, National Center of Neurology and Psychiatry, 4-1-1, Ogawa-Higashi, Kodaira, Tokyo 187-8502, Japan
[b] Department of Radiology, National Center of Neurology and Psychiatry, 4-1-1, Ogawa-Higashi, Kodaira, Tokyo 187-8551, Japan
[c] Department of Imaging Neuroinformatics, Integrative Brain Imaging Center, National Center Hospital of Neurology and Psychiatry, 4-1-1 Ogawa-Higashi, Kodaira, Tokyo 187-8502, Japan
[d] Department of Neurology, National Center of Neurology and Psychiatry, 4-1-1, Ogawa-Higashi, Kodaira, Tokyo 187-8551, Japan
[e] Department of Psychiatry, National Center of Neurology and Psychiatry, 4-1-1, Ogawa-Higashi, Kodaira, Tokyo 187-8551, Japan
[f] Department of Immunology, National Institute of Neuroscience, National Center of Neurology and Psychiatry, 4-1-1, Ogawa-Higashi, Kodaira, Tokyo 187-8502, Japan

ARTICLE INFO

Article history:
Received 20 September 2012
Revised 30 January 2013
Accepted 9 March 2013

Keywords:
Cerebral blood flow
Multiple sclerosis
Pseudocontinuous arterial spin labeling
T2-hyperintense lesion

ABSTRACT

Arterial spin labeling (ASL) is a noninvasive technique that can measure cerebral blood flow (CBF). To our knowledge, there is no study that examined regional CBF of multiple sclerosis (MS) patients by using this technique. The present study assessed the relationship between clinical presentations and functional imaging data in MS using pseudocontinuous arterial spin labeling (pCASL). Twenty-seven patients with MS and 24 healthy volunteers underwent magnetic resonance imaging and pCASL to assess CBF. Differences in CBF between the two groups and the relationships of CBF values with the T2-hyperintense volume were evaluated. Compared to the healthy volunteers, reduced CBF was found in the bilateral thalami and right frontal region of the MS patients. The volume of the T2-hyperintense lesion was negatively correlated with regional CBF in some areas, such as both thalami. Our results suggest that demyelinated lesions in MS mainly have a remote effect on the thalamus and that the measurement of CBF using ASL could be an objective marker for monitoring disease activity in MS.

1. Introduction

Multiple sclerosis (MS) is a common autoimmune disorder of the central nervous system (CNS) characterized by inflammatory demyelination and secondary axonal degeneration. Although MS has classically been thought of as a typical white matter disorder, the involvement of gray matter regions in the demyelinating process was acknowledged in early pathology studies [1–5], and some hypotheses have been put forward that have explored possible pathogenic processes leading to gray matter damage. These processes could be either primary (arising within gray matter regions) or secondary (pathological changes in gray matter regions that result from continuing damage in the cerebral white matter) and might be intricately connected with each other [6].

Positron emission tomography (PET), single photon emission computed tomography (SPECT) and dynamic susceptibility contrast (DSC)-enhanced magnetic resonance imaging (MRI) have been used to investigate cerebral metabolic rate, cerebral blood flow (CBF) and cerebral perfusion in MS, respectively. Such imaging techniques have shown significant decreases in areas of white matter, cortical gray matter, subcortical gray matter and normal-appearing white matter [7–16]. However, due to the dissemination of MS lesions in space and time, potential markers for determining their outcomes are poorly understood.

Arterial spin labeling (ASL) MRI is a noninvasive technique that can measure CBF. ASL MRI has two major categories: continuous ASL (CASL) and pulsed ASL (PASL) [17]. The CASL technique uses continuous adiabatic inversion, whereas PASL uses a single inversion pulse. Due to the long steady-state tagging, this technique often has high power disposition and sometimes requires a second radio-frequency (RF) coil for spin labeling [18,19]. Therefore, it has not been widely used compared with PASL, which is simpler in implementation. The recently developed pseudocontinuous ASL (pCASL) MRI is an intermediate technique between CASL and PASL [20–22]. This technique uses a series of discrete RF pulses to mimic the CASL method for spin labeling and brings the potential of combining the

☆ Conflict of interest: None.

* Corresponding author. Tel.: +81 42 341 2712; fax: +81 42 346 2094.
E-mail address: ota@ncnp.go.jp (M. Ota).

0730-725X/$ – see front matter © 2013 Elsevier Inc. All rights reserved.
http://dx.doi.org/10.1016/j.mri.2013.03.016

merits of PASL, including less hardware demand and higher tagging efficiency, and CASL, which include a longer tagging bolus and thus a higher signal-to-noise ratio.

ASL measures CBF by taking advantage of arterial water as a freely diffusible tracer, avoiding the need for gadolinium or radioactive ligands; thus, ASL would be a noninvasive and repeatable method of measuring CBF. The ASL technique could be used in place of DSC, PET and SPECT for the examination of neurologic disorders.

We hypothesized that decreased CBF measured by pCASL would, in reflecting neuronal and axonal loss, be associated with the clinical course and disabling forms of MS. In the present study, we assessed the relationship between clinical presentations and functional imaging data in MS using pCASL.

2. Material and methods

2.1. Participant selection

The subjects were 27 patients with MS and 24 healthy controls matched for age, gender and whole brain volume. MS was diagnosed by using previously defined criteria [23]. One female patient out of 27 was the primary progressive MS, and 8 out of 27 (all of them were female, mean age = 47.3 ± 12.9 years) were the secondary progressive MS. No subject had a previous history of any other significant central nervous or systemic autoimmune conditions. The healthy controls were all volunteers without any confirmed neuropsychiatric or major medical illness. All MS subjects underwent a neurological examination to evaluate their Expanded Disability Status Scale (EDSS) scores [24]. The demographic and clinical data of the subjects are shown in Table 1. The study protocol was approved by the Ethics Committee of the National Center of Neurology and Psychiatry, Japan. Informed consent for participation in the study was obtained from all subjects.

2.2. MRI data acquisition and processing

Experiments were performed on a 3-T MR system (Philips Medical Systems, Best, the Netherlands). High spatial resolution, 3-dimensional (3D) T1-weighted images were used for morphometric study. 3D T1-weighted images were acquired in the sagittal plane [repetition time (TR)/echo time (TE), 7.18/3.46; flip angle, 10°; effective section thickness, 0.6 mm; slab thickness, 180 mm; matrix, 384 × 384; field of view (FOV), 261 × 261 mm; number of signals acquired, 1], yielding 300 contiguous slices through the brain. In addition to 3D T1-weighted images, we acquired axial T2-weighted turbo spin echo images (TR/TE, 4507/80; slice thickness, 3 mm; intersection gap, 1.5 mm; matrix, 640 × 640; FOV, 230 × 230 mm; number of signals acquired, 1) and axial fluid-attenuated inversion recovery (FLAIR) images (TR/TE/inversion time, 10,000/120/2650 ms; slice thickness, 3 mm; intersection gap, 1.5 mm; matrix, 512 × 512; FOV, 230 × 230 mm; number of signals acquired, 1). The imaging parameters for all of the pCASL experiments were identical: single-shot gradient-echo echo planar imaging (EPI) in combination with parallel imaging (SENSE factor 2.0), FOV = 240 × 240, matrix =64 × 64, voxel size = 3.75 × 3.75 mm, 20 slices acquired in ascending order, slice thickness = 7 mm, 1-mm gap between slices, labeling duration = 1650 ms, post spin labeling delay = 1520 ms, TR =4000 ms, TE = 12 ms, time interval between consecutive slice acquisitions = 32.0 ms, RF duration = 0.5 ms, pause between RF pulses = 0.5 ms, labeling pulse flip angle = 18°, bandwidth = 3.3 kHz/pixel, echo train length = 35. Thirty-two pairs of control/label images were acquired and averaged. The scan duration was 4:24. For measurement of the magnetization of arterial blood and also for segmentation purposes, an EPI M0 image was acquired separately with the same geometry and the same imaging parameters as the pCASL without labeling.

Table 1
Characteristics of the study sample.

	Healthy volunteers	Multiple sclerosis patients
Male/female	7/17	7/20
Age	38.3 ± 13.2	42.7 ± 13.6
Whole brain volume (L)	1.1 ± 0.1	1.1 ± 0.1
Duration of illness		10.6 ± 9.2
EDSS		4.4 ± 2.5
T2-hyperintense lesion volume (cm^3)		3.4 ± 4.0

2.3. Postprocessing of the ASL data

Because pCASL and M0 images were acquired separately, both image signal intensities were corrected for data scaling. Corrected data were transferred to a workstation and analyzed using ASLtbx software working on Matlab (Math Works, Natick, MA, USA) [25]. For the CBF calculations, we added the attenuation correction for the transversal relaxation rate of gray matter to the original equation as shown:

$$\begin{aligned}\mathrm{CBF\,(ml/100\,g/min)} &= (6000 * \mathrm{delM} * \mathrm{lamb}) \\ &\quad * \exp(\mathrm{TE}/T^*_{2.\mathrm{gm}}/[2 * \mathrm{alp} * T_{1,\mathrm{blood}} * \mathrm{M0WM}\{\exp(-w/T_{1,\mathrm{blood}}) \\ &\quad -\exp\left(-(\mathrm{tau}+w)/T_{1,\mathrm{blood}}\right)\}],\end{aligned}$$

Where delM is the difference signal between the control and label acquisitions, lamb is the blood/tissue water partition coefficient, $T_{1,\mathrm{blood}}$ is the longitudinal relaxation time of blood, tau is the labeling time, w is the post labeling delay time, TE is the echo time and $T^*_{2.\mathrm{gm}}$ is the transversal relaxation time of gray matter (assumed to be 44.2 ms) [26]. Alp is the labeling efficiency, and M0WM is the average intensity in the control image within the white matter that was derived from the segmented M0 white matter image calculated using Statistical Parametric Mapping 5 software (SPM5; Wellcome Department of Imaging Neuroscience, London, UK) running on Matlab 7.0. The parameters used in this study were alp = 0.85 (assumed) [17], $T_{1,\mathrm{blood}}$ = 1664 ms (assumed) [27], λ = 0.9 g/ml (assumed) [28], tau = 1.65 s (calculated) and w = 1525 (calculated) ms.

The mean CBF image derived using the ASLtbx software contained some spike noise, and thus, a median filter (a nonlinear digital filtering technique) was used in this study. In median filtering, the neighboring pixels are ranked according to the intensity, and the median value becomes the new value for the central pixel. Since the slice gap that we used was somewhat large, simple 2D median filtering was used. Fig. 1 illustrated the image from the ASL sequence in a single subject. To evaluate CBF voxel-basically, mean CBF images were normalized to the standard space. On the occasion of normalization, each individual 3D-T1 image was first coregistered and resliced to its own M0 image. Next, the coregistered 3D-T1 image was normalized to the "avg152T1" image regarded as the anatomically standard image in SPM5, and then the transformation matrix was applied to the FA maps to normalize them to the standard space. The spatially normalized images were resliced with a final voxel size of approximately 4 × 4 × 8 mm^3. Each map was then spatially smoothed with a 4-mm full-width at half-maximum Gaussian kernel in order to decrease spatial noise and compensate for the inexactitude of normalization.

2.4. Measure of volume of T2-hyperintense lesion

The T2-weighted data and FLAIR images for each subject were transferred to the workstation. To measure the accurate volume of the T2-hyperintense lesion, individual T2-weighted data and FLAIR